Supporting Information for

High-resolution Tb^{3+}-doped Gd-based oxyfluoride glass scintillators for X-ray imaging

LianJie Li[a], JunYu Chen[a], XiuSha Peng[a], TingMing Jiang[b], Lei Lei[a*], Hai Guo[a*]

[a]Department of Physics, Zhejiang Normal University, Jinhua, Zhejiang, 321004, China

[b]State Key Laboratory of Modern Optical Instrumentation, Zhejiang University, Hangzhou, 310027, China

[*]**Corresponding author:**
Lei Lei, E-mail: leilei@cjlu.edu.cn
Hai Guo, E-mail: ghh@zjnu.cn

A. Details of XEL spectrometer

The XEL correlation spectra were obtained using the OmniFluo960 X-ray fluorescence spectrometer of Zolix Company. The detector used in the spectrometer is PMTH-S1-(CR131) series side window type photomultiplier tube. The cathode sensitivity and cathode illumination sensitivity of the photomultiplier tube are 74 mA/W and 140 μA/Lm, respectively. The sample exposed to X-rays during measurement was a circular plane with a diameter of 10 mm.

The top view of the excitation cell structure of the X-ray fluorescence spectrometer is shown in Fig. S1. The X-rays generated by the X-ray source irradiates the sample surface under the angle of 45°, while the angle difference between the photomultiplier tube and the normal of the sample surface is also 45°.

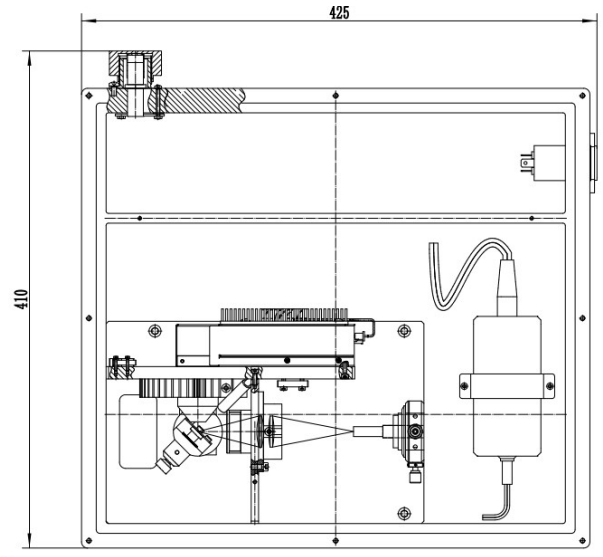

Fig. S1 Top view of the excitation cell structure of the X-ray fluorescence spectrometer.

B. Detail information of BGO crystal

The BGO crystal was purchased from Shanghai Institute of Ceramics, Chinese Academy of Sciences, which is one of best quality suppliers of BGO crystal. The specific parameters were listed in following Table S1. Besides, PL and PLE spectra of BGO and SiBNaBaGd-5.0Tb sample are displayed in Fig. S2(a-b).

Table S1 Parameters of BGO crystal from Shanghai Institute of Ceramics, Chinese Academy of Sciences.

Parameter	Value
Density (g/cm^3)	7.13
Radiation length (cm)	1.12
Decay constant (ns)	300
Emission peak (nm)	480
Light output (ph/MeV)	8000-9000
Melting point (℃)	1050
Hardness (Mho)	5
Refractive Index	2.15
Hygroscopicity	none
Cleavage	none

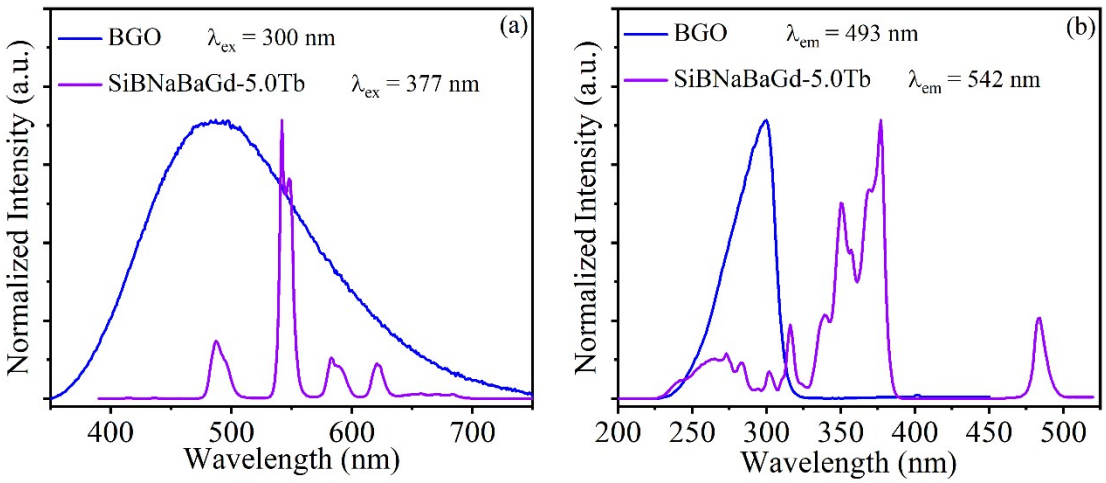

Fig. S2 (a) PL and (b) PLE spectra of BGO and SiBNaBaGd-5.0Tb sample.

C. Calculation of X-ray excited luminescence intensities

Integrated X-ray excited luminescence (XEL) intensities ($I_{\text{R-XEL}}$) were calculated by the following equation,

$$I_{\text{R-XEL}} = \frac{I_{\text{glass-XEL}}}{I_{\text{BGO-XEL}}} = \frac{\int_{300}^{750} I_{\text{sample}}(\lambda)\mathrm{d}\lambda}{\int_{300}^{750} I_{\text{BGO}}(\lambda)\mathrm{d}\lambda} \quad \text{(S1)}$$

where $I_{\text{R-XEL}}$ is the ratio of luminescent intensity of glass samples to BGO, $I_{\text{glass-XEL}}$ and $I_{\text{sample}}(\lambda)$ are the XEL intensity of glass samples, $I_{\text{BGO-XEL}}$ and $I_{\text{BGO}}(\lambda)$ are the XEL intensity of BGO. The XEL intensities of SiBNaBaGd-*x*Tb (*x* = 1.0, 2.0, 3.0, 4.0, 4.5 and 5.0) samples are 117%, 145%, 167%, 191%, 238% and 250% of that of BGO, respectively.

D. Schematic diagram of equipment for X-ray imaging

To assess the X-ray imaging performance of SiBNaBaGd-5.0Tb glass, X-ray images of a chip, a capsule containing a spring and standard X-ray resolution test pattern plate were taken by home-made equipment for X-ray imaging, as shown in Fig. S3.

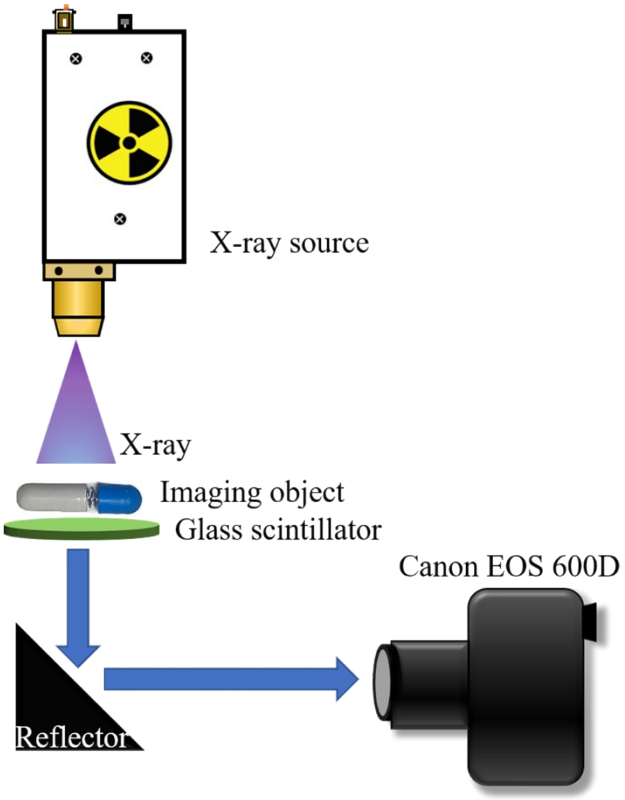

Fig. S3 Schematic diagram of the home-made equipment for X-ray imaging.

E. Calculation of error bars

Considering the experimental uncertainty, the transmittance (*T*), average lifetimes of Tb^{3+} and Gd^{3+}, and internal quantum efficiency (IQE) were measured five times. The error bars were computed by following equation,

$$s = \pm\sqrt{\sum_{i=1}^{n}\left(x_i - \bar{x}\right)^2 \Big/ \left(n-1\right)} \quad \text{(S2)}$$

where *s* represents variance, x_i represents test value, *x* represents average value and *n* (*n* = 1-5) represents test times. The smaller the standard deviation, the more stable the test results. As illustrated in Fig. S(4-7), the results of each test were marked in figures. Besides, the results, average values and standard deviations of transmittance (*T*), average lifetimes of Tb^{3+} and Gd^{3+}, and internal quantum efficiency (IQE) are listed in Table S(2-5).

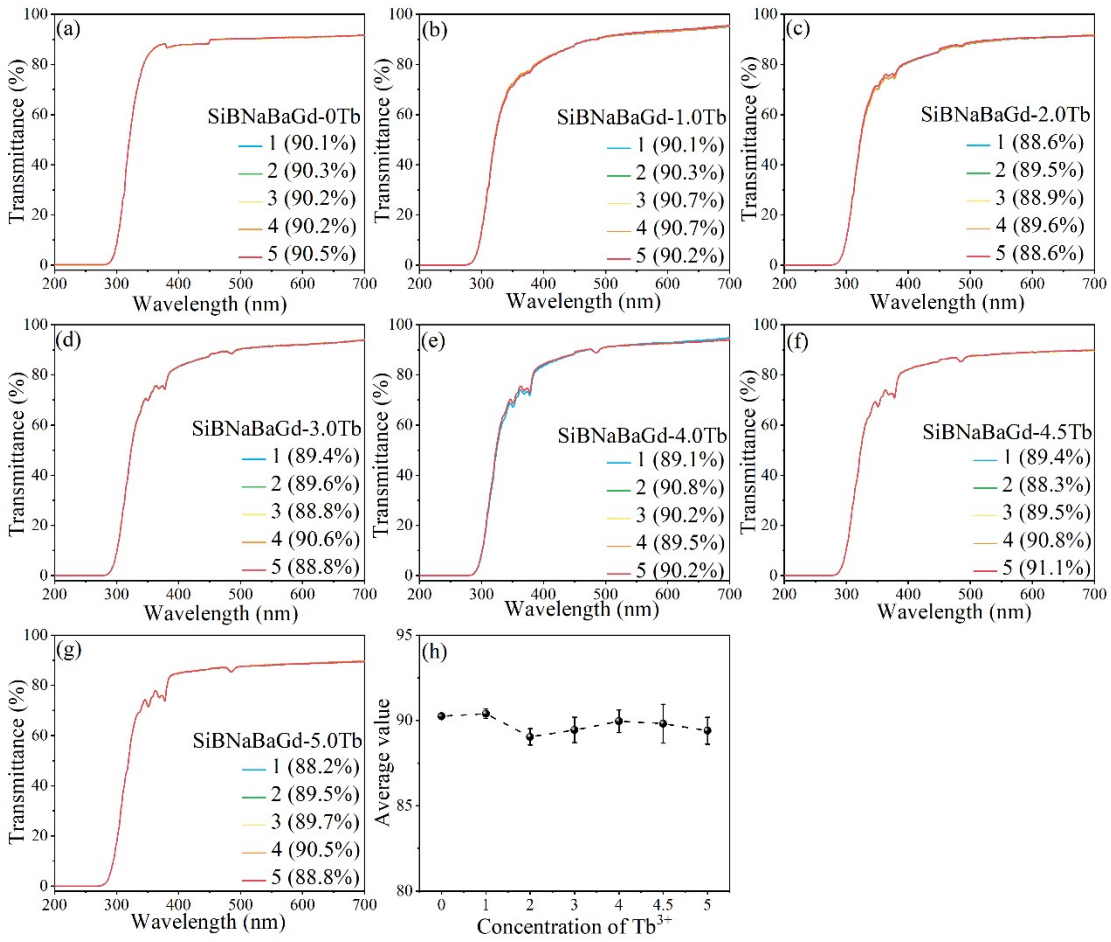

Fig. S4 (a-g) Transmission spectra of SiBNaBaGd-*x*Tb samples and (h) the error bars spectra of *T*.

Table S2 The results, average values and standard deviations of *T*.

Test times / Tb^{3+} content	1	2	3	4	5	Average value	σ
0Tb	90.1	90.3	90.2	90.2	90.5	90.3	0.2
1Tb	90.1	90.3	90.7	90.7	90.2	90.4	0.3
2Tb	88.6	89.5	88.9	89.6	88.6	89.0	0.5
3Tb	89.4	89.6	88.8	90.6	88.8	89.4	0.7
4Tb	89.1	90.8	90.2	89.5	90.2	89.9	0.7
4.5Tb	89.4	88.3	89.5	90.8	91.1	89.8	1.0
5Tb	88.5	89.5	89.7	90.5	88.8	89.4	0.8

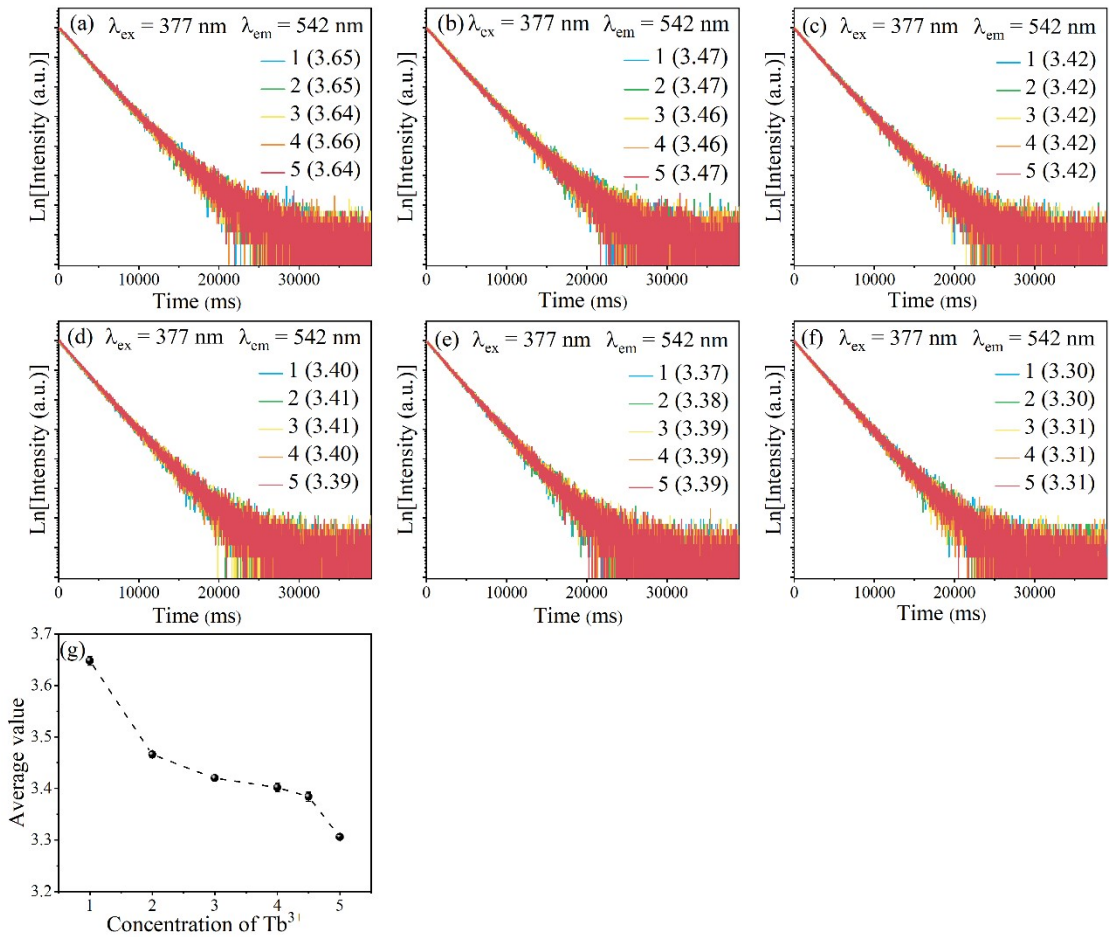

Fig. S5 (a-f) Decay curves of emission at 542 nm (λ_{ex} = 377 nm) of SiBNaBaGd-*x*Tb samples and (g) the error bars spectra of average lifetimes of Tb^{3+}.

Table S3 The results, average values and standard deviations of average lifetimes of Tb^{3+}.

Tb^{3+} content \ Test times	1	2	3	4	5	Average value	σ
1Tb	3.65	3.65	3.64	3.66	3.64	3.65	0.01
2Tb	3.47	3.47	3.46	3.46	3.47	3.47	0.01
3Tb	3.42	3.42	3.42	3.42	3.42	3.42	0.00
4Tb	3.40	3.41	3.41	3.40	3.39	3.40	0.01
4.5Tb	3.37	3.38	3.39	3.39	3.39	3.38	0.01
5Tb	3.30	3.30	3.31	3.31	3.31	3.31	0.01

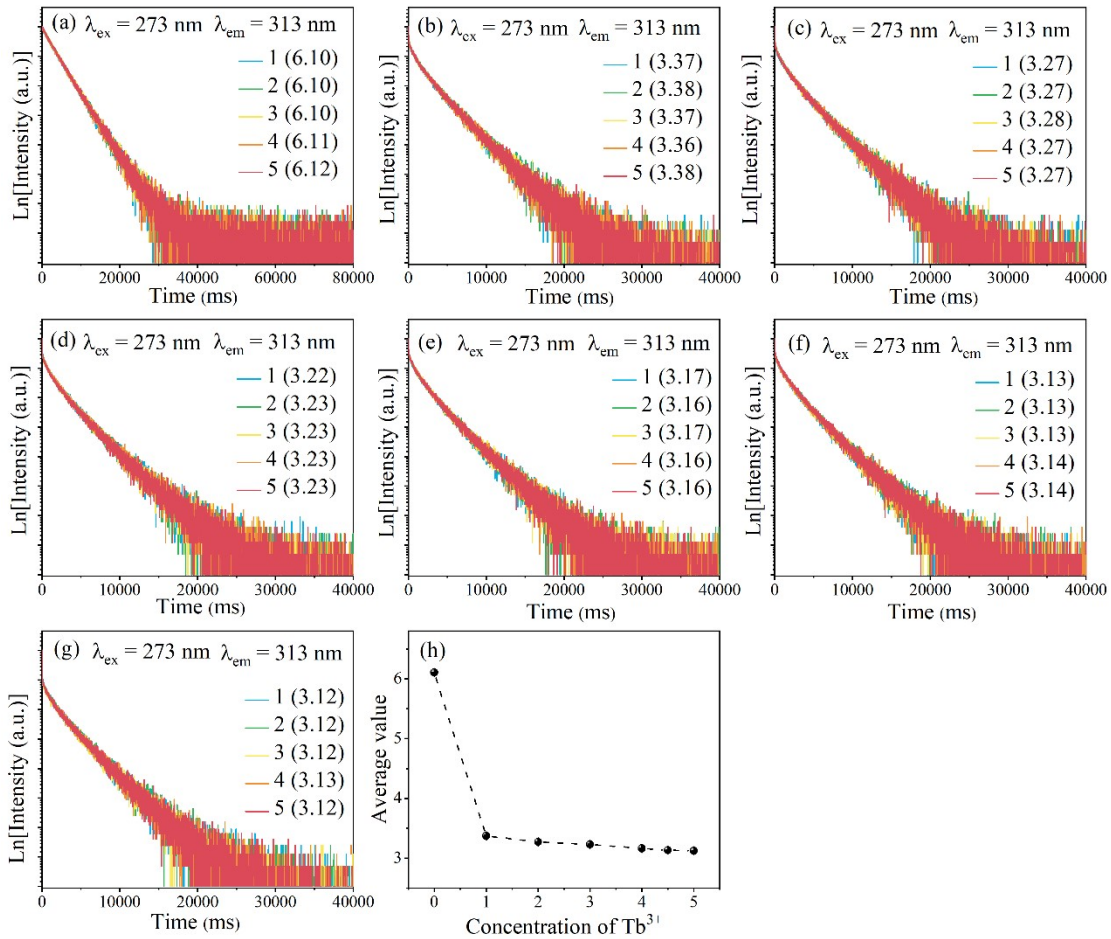

Fig. S6 (a-g) Decay curves of emission at 313 nm (λ_{ex} = 273 nm) of SiBNaBaGd-*x*Tb samples and (h) the error bars spectra of average lifetimes of Gd^{3+}.

Table S4 The results, average values and standard deviations of average lifetimes of Gd^{3+}.

Tb^{3+} content \ Test times	1	2	3	4	5	Average value	σ
0Tb	6.10	6.10	6.10	6.11	6.12	6.11	0.01
1Tb	3.37	3.38	3.37	3.36	3.38	3.37	0.01
2Tb	3.27	3.27	3.28	3.27	3.27	3.27	0.01
3Tb	3.22	3.23	3.23	3.23	3.23	3.23	0.01
4Tb	3.17	3.16	3.17	3.16	3.16	3.16	0.01
4.5Tb	3.13	3.13	3.13	3.14	3.14	3.13	0.01
5Tb	3.12	3.12	3.13	3.12	3.12	3.12	0.01

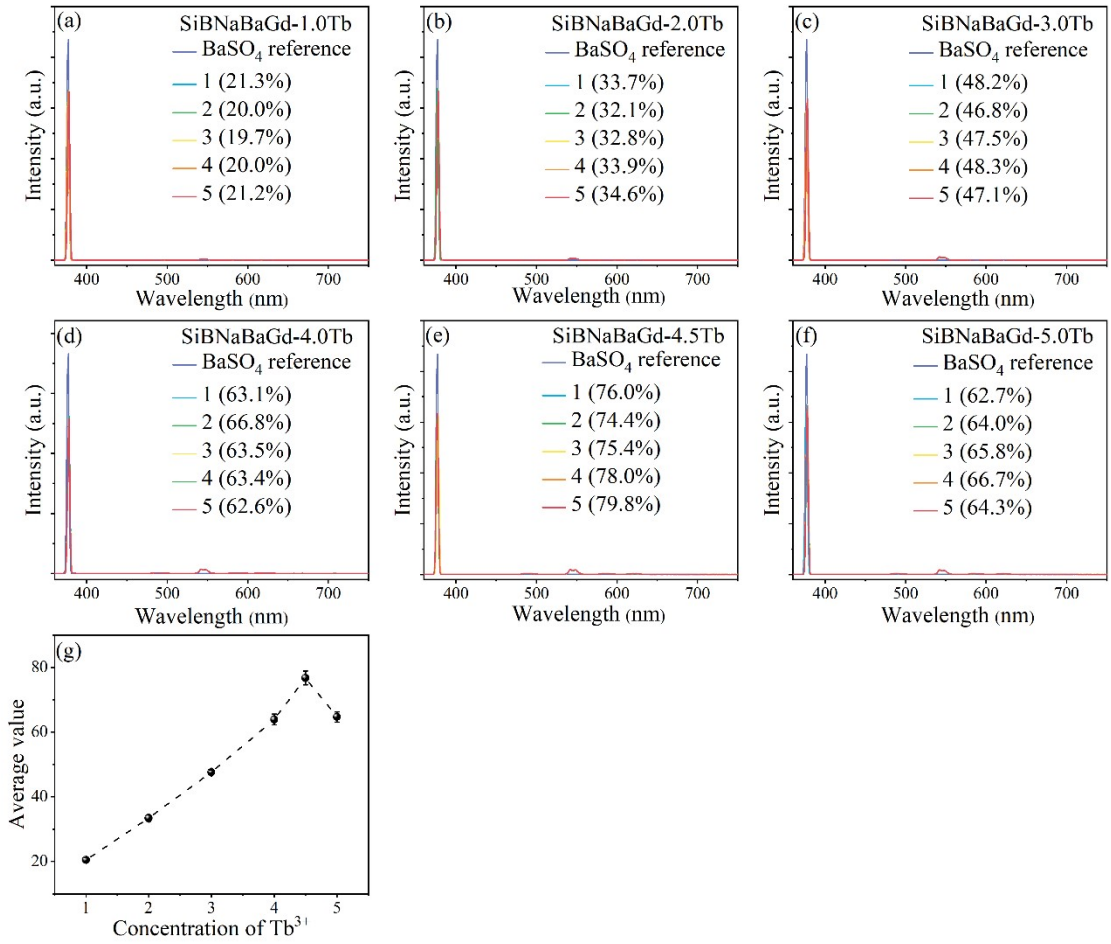

Fig. S7 (a-f) Excitation lines of $BaSO_4$ reference, and PL (λ_{ex} = 377 nm) spectra of SiBNaBaGd-*x*Tb and (g) the error bars spectra of IQE.

Table S5 The results, average values and standard deviations of IQE.

Tb^{3+} content \ Test times	1	2	3	4	5	Average value	σ
1Tb	21.3	20.0	19.7	20.0	21.2	20.4	0.8
2Tb	33.7	32.1	32.8	33.9	34.6	33.4	1.0
3Tb	48.2	46.8	47.5	48.3	47.1	47.6	0.7
4Tb	63.1	66.8	63.5	63.4	62.6	63.9	1.7
4.5Tb	76.0	74.4	75.4	78.0.	79.8	76.7	2.0
5Tb	62.7	64	65.8	66.7	64.3	64.7	1.6

F. XRD patterns of SiBNaBaGd-*x*Tb samples

The XRD patterns of SiBNaBaGd-*x*Tb (x = 0, 1.0, 2.0, 3.0, 4.0, 4.5 and 5.0) specimens are figured in Fig. S8. These XRD patterns are consisted of two diffuse humps, confirming the amorphous nature of SiBNaBaGd-*x*Tb specimens.

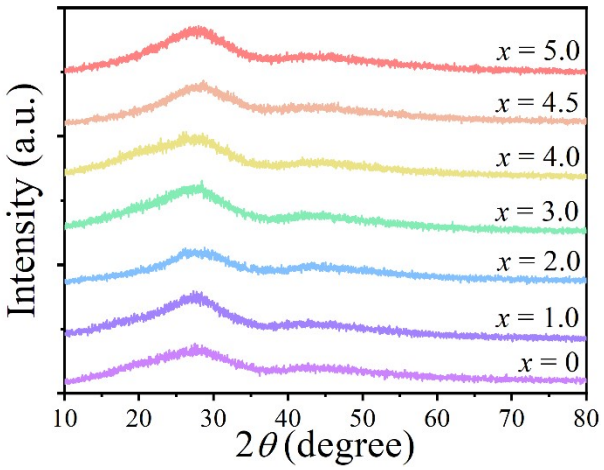

Fig. S8 XRD patterns of SiBNaBaGd-*x*Tb samples.

G. Results of compositional analysis

Considering the effect of corundum crucible on composition of samples and the evaporation of B and F, the compositional analyses of SiBNaBaGd host and SiBNaBaGd-5.0Tb sample were measured by X-Ray fluorescence. And the relating results are listed in Table S6.

It can be observed that the increased contents of Al are 5.42 and 5.62 wt% for SiBNaBaGd host and SiBNaBaGd-5.0Tb sample, respectively. That is to say, the contamination from corundum crucible has little influence on the compositions of samples. Besides, B and F evaporate during the glass melting process, but the amount of evaporation is very small. As can be seen from the Table S6, the measured content F was reduced by less than 0.9 wt% compared to theoretical contents. Due to the limitation of XRF spectroscopy, the content of B cannot be measured. In conclusion, the composition of samples is basically unchanged and the preparation of glass samples in Al_2O_3 crucible is repeatable.

Table S6 Element contents of SiBNaBaGd host and SiBNaBaGd-5.0Tb sample.

Element (wt%)	Host		5Tb	
	theoretical	measured	theoretical	measured
Si	19.65	22.10	19.63	21.57
B	3.24	/	3.24	/
Na	10.34	11.15	10.33	10.81
Ba	13.73	12.58	13.71	12.98
Gd	11.79	11.05	1.96	1.86
Tb	0.00	0	9.92	9.63
F	8.07	7.26	8.06	7.25
Al	0.00	5.42	0.00	5.62

H. Comparison of XEL intensity of SiBNaBaGd-*x*Tb (*x* = 5.0, 5.5 and 6.0) samples

In order to demonstrate the best XEL performance of SiBNaBaGd-5.0Tb, experiments of glass scintillators doped with higher concentration of Tb^{3+} were supplemented, and their XEL spectra were tested. As shown in Fig. S9, the XEL intensities of SiBNaBaGd-*x*Tb (*x* = 5.0, 5.5 and 6.0) samples are 250%, 225% and 169% of that of $B_4G_3O_{12}$ (BGO), respectively. Therefore, SiBNaBaGd-5.0Tb sample represents optimal XEL intensity and was selected for further investigation.

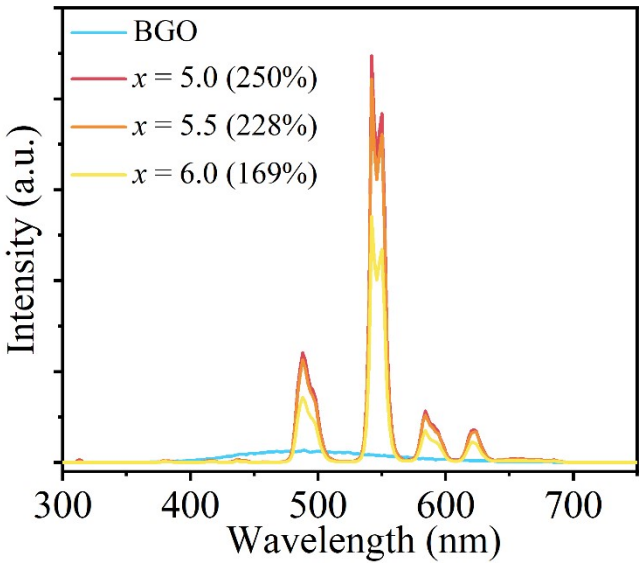

Fig. S9 XEL spectra of SiBNaBaGd-*x*Tb (*x* = 5.0, 5.5 and 6.0) samples and BGO crystal excited by X-ray.

I. Comparison of transmittance before and after irradiation

Transmittance spectra of SiBNaBaGd-5.0Tb samples before and after 150 min X-ray irradiation and irradiated SiBNaBaGd-5.0Tb sample followed with heat-treatment at 300 ℃ for 2 h are exhibited in Fig. S10. It can be seen that the transmittance at 542 nm still exceeds 84% for SiBNaBaGd-5.0Tb sample after 150 min X-ray irradiation. The radiated SiBNaBaGd-5.0Tb sample followed with heat-treatment shows good transparency as sample before irradiation.

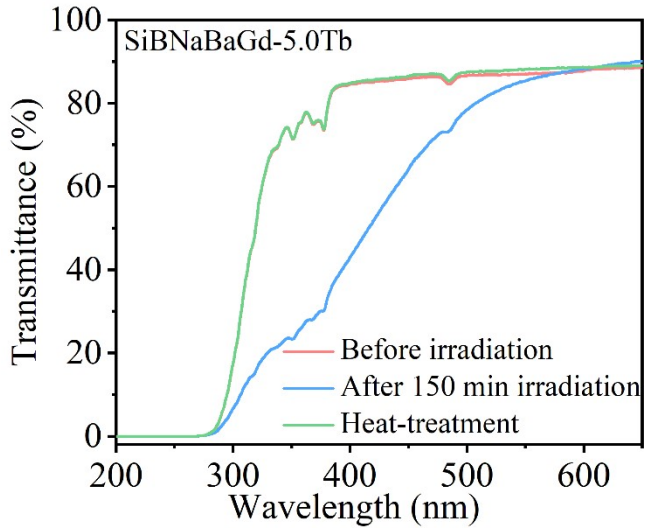

Fig. S10 Transmission spectra of SiBNaBaGd-5.0Tb sample before and after 150 min X-ray irradiation and after heat-treatment for 2 h.